Bifurcation in the Friedberg-Lee model

1991 J. Phys. A: Math. Gen. 24 2977

(http://iopscience.iop.org/0305-4470/24/13/014)

J. Phys. A: Math. Gen. 24 (1991) 2977-2993. Printed in the UK

Bifurcation in the Friedberg–Lee model

M A Lohe†

Department of Physics, Duke University, Durham, NC 27706, USA

Received 3 December 1990

Abstract. We investigate solutions of the Friedberg–Lee model in which the soliton bag is defined on a small domain determined by a radius R. Such solutions arise when the nucleon is modelled as a soliton bag and, when compressed within the nucleus, is confined to a domain of the order of the soliton size itself. By means of linear analysis we show that at a certain value of R the soliton solutions bifurcate from constant solutions. This enables us to determine solution branches for small R, and the values of R for which the soliton bag has lower energy than that of the constant solution. The discontinuity where the branches cross can be viewed in the quantum theory as a transition from a nucleon state to a uniform plasma. We also find multi-soliton solutions and kink solitons which bifurcate from a different constant solution. We describe a numerical method which allows us to follow solutions from the bifurcation radius as R is varied and we apply the method to obtain numerical solutions for small R.

1. Introduction

The aim of soliton bag models is to reproduce the properties of the low-lying hadronic states not presently calculable directly from QCD. A recent account of work carried out on such models has been provided by Wilets [1]. In the Friedberg–Lee model [2, 3], the simplest of the non-topological models, there is only one scalar field σ, identified with the gluon condensate, which interacts with quark fields ψ. The model is solved in the mean field approximation, in which σ becomes a static classical field and the quark fields ψ are expanded in terms of a complete set of spinor basis functions with fermion operator coefficients. The quantum field equations are in this way reduced to a system of nonlinear partial differential equations, with boundary conditions determined by the requirements of finite energy. From the solutions baryon wavefunctions can be constructed and quantities of physical interest, such as the mass and charge radius of the nucleon, can be calculated. Higher order corrections and other modifications are described by Wilets [1]. Although the Friedberg–Lee model does not provide a realistic description of nuclear matter, since for example it lacks chiral symmetry, the techniques we use here to investigate nucleon behaviour within this model are general, and will be applicable to more realistic models, such as the chromo-dielectric model described by Wilets [1].

Given the model of individual nucleons as solitons one would like to model the nucleus by assembling many solitons together, perhaps in a lattice configuration, to form the nucleus. Since the solitons could overlap it is necessary to modify the boundary conditions from the single soliton case to ensure that adjacent solitons join smoothly.

† Permanent address: Northern Territory University, PO Box 40146, Casuarina NT 0811, Australia.

0305-4470/91/132977+17$03.50

In this context, the solitons will exist on a small domain of the order of the soliton size itself, and we are therefore led to investigate their properties on a small domain determined by a radius R which is allowed to vary. In the Wigner-Seitz approximation each soliton occupies a cell equivalent in volume to a sphere of radius R and is assumed to be spherically symmetric. As R becomes very small the soliton is compressed and begins to lose its soliton identity; in fact at a certain radius we show that it reduces to the constant solution, which in the quantum theory corresponds to a uniform plasma of fermion and scalar fields. By investigating the effect on the soliton of varying R we expect therefore to obtain information on the nature of the transition from the nucleon to the plasma state.

The fact that the quantum field equations are reduced to a system of coupled ordinary differential equations means that well established techniques can be applied to analyse and solve these equations, and determine qualitative behaviour which might be common to a range of models. In particular, we apply bifurcation analysis to the Friedberg-Lee model to investigate the dependence of the solution on R. For small R the soliton solution does not exist, but at a certain value R_1 the soliton bag bifurcates from a constant solution, and for large R has lower energy and so is the preferred state. The existence of the bifurcation is detected by linear analysis of the nonlinear field equations, and we use a numerical method [4] which enables us to follow the soliton branch as R is varied. We investigate here the case in which the fermions are all placed in the ground state, so our analysis only applies directly for solitons in the zero temperature limit. However, we expect that similar bifurcation behaviour will exist for the general case in which the lowest levels of the fermion band are filled. This is demonstrated in [5] for the one-dimensional version of the Friedberg-Lee model, by finding an exact solution which is valid for an arbitrary packing of the fermion band and for an arbitrary number of cells. Provided the top level of the band is unfilled the bifurcation proceeds in the same way as for the case in which only the lowest level is occupied.

The first step in analysing the bifurcation behaviour is to classify all constant solutions, and this is done in section 3. The two classes of solution lead to two soliton types, the soliton bag and kink solitons which resemble the kinks of one-dimensional models. By linearizing about the constant solutions we find necessary conditions for the existence of bifurcating branches. Bifurcation can occur only for certain values of R which are determined algebraically, and the quark eigenvalue and total field energy are also determined exactly, as shown in section 3. The soliton bag bifurcates from a constant solution which in the quantum theory can be viewed as a uniform fermion-scalar field plasma. In section 4 we analyse the case of solutions bifurcating from a different constant solution, one which in the quantum theory corresponds to an unstable vacuum for the scalar field sector. In section 5 we present a numerical method for finding solutions to the full nonlinear equations by following a solution branch from its bifurcation point, and apply the method to find actual solutions near the bifurcation point, keeping fixed the quark eigenvalue. It remains to carry out a thorough numerical investigation keeping the physical parameters of the model fixed.

It is instructive to examine the bifurcation behaviour in a simple soliton model and so in section 2 we demonstrate that sine-Gordon solitons bifurcate from the constant solution as the domain $[-R, R]$ is increased. For this model, and that with a quartic potential, exact solutions can be found and their behaviour analysed explicitly; however the solutions are relevant only classically, since the solitons join only to anti-solitons and so will annihilate quantum mechanically. The property of bifurcation as R is varied is common to other soliton models, including topological solitons such as vortices and magnetic monopoles.

2. One-dimensional models

In one space dimension, a well-studied class of soliton models has properties determined by the equation (for the static case)

$$\sigma'' = \frac{dU(\sigma)}{d\sigma} \tag{2.1}$$

where $U(\sigma)$ is a suitable potential, and $' \equiv d/dx$. We wish to assemble static solitons together on the line and so an individual soliton is defined on the interval $[-R, R]$ for some finite R, and we impose the boundary conditions

$$\sigma'(R) = 0 = \sigma'(-R) \tag{2.2}$$

which ensure that adjacent solitons join smoothly. For the case of a single soliton located at the origin, σ is odd in x, $\sigma(x) = -\sigma(-x)$, and then we need solve (2.1) only on $[0, R]$ with the boundary conditions $\sigma'(R) = 0 = \sigma(0)$. In order to exhibit the dependence of the solution on R, define $s = x/R$, so that for the sine–Gordon model, for which $U(\sigma) = \cos\sigma$,

$$\ddot{\sigma} = -R^2 \sin\sigma \tag{2.3}$$

with $\dot{\sigma}(-1) = 0 = \dot{\sigma}(1)$, where $\dot{\sigma} \equiv d\sigma/ds$. The behaviour of the solution as R is varied is well known from the studies of the *elastica*, the model for a beam buckling under compression considered by Euler and Bernoulli. A description is provided by Reiss in [6, p7], also by Chow and Hale [7, p 5]. In the classical problem an elastic rod of certain length is subject to a compressive force which eventually buckles the rod. The unknown σ is the angle which the unit tangent vector to the rod makes under buckling, and the variable s is the arclength along the rod. This buckling can be viewed as a bifurcation of a non-trivial solution from the trivial solution $\sigma = 0$ of (2.3) as the bifurcation parameter, the applied force, is increased. In our problem 'compression' means reducing R in (2.3), whereas in the Euler–Bernoulli problem it means increasing the coefficient on the right-hand side of (2.3), which is proportional to the applied force.

The picture we obtain, in terms of solitons, is that for small R only the trivial solution of (2.3) $\sigma = 0$ exists but when R is increased to a certain value $R = R_1$, a soliton bifurcates from $\sigma = 0$ and in the limit $R \to \infty$ becomes the familiar one-soliton solution of the sine–Gordon equation. There are also bifurcation points for larger values of R, $R = R_n$ for $n = 2, 3, \ldots$, which describe n-soliton solutions, and which also bifurcate from the trivial solution $\sigma = 0$. These solutions can be viewed as n single solitons located next to each other on the real line.

This behaviour can be precisely described by integrating (2.3), with the solutions appearing as elliptic functions. Since details appear in [6] let us instead write out the solution for the quartic potential

$$U(\sigma) = \tfrac{1}{2}(1 - \sigma^2)^2. \tag{2.4}$$

(There is similar behaviour for any potential which admits soliton solutions.) One integration of (2.1) gives

$$\tfrac{1}{2}(\sigma')^2 = U(\sigma) - U(\sigma_R) \tag{2.5}$$

where $\sigma_R = \sigma(R)$. A further integration using (2.4) gives

$$\sigma(x) = \sigma_R \operatorname{sn}(x\sqrt{2-\sigma_R^2}, k) \tag{2.6}$$

where $k = \sigma_R/\sqrt{2-\sigma_R^2}$ with $0 \leq k < 1$ and $\operatorname{sn}(u, k)$ is the Jacobian elliptic function. (See Abramowitz and Stegun [8] for a definition and properties.) Next we impose $\sigma(R) = \sigma_R$, to obtain

$$R\sqrt{2-\sigma_R^2} = (2n-1)K(k) \tag{2.7}$$

where K is the complete elliptic integral of the first kind and n is an integer. Here we have used the fact that $\operatorname{sn}(u, k) = 1$ at $u = K(k)$, $5K(k) \ldots$ and we can also include the cases $u = 3K(k)$, $7K(k) \ldots$ since these also describe multi-kink solutions, odd in x. Given R, (2.7) determines σ_R, with $0 \leq \sigma_R < 1$ and then $\sigma(x)$ is given by (2.6). For $R \to \infty$ we regain the familiar kink solution $\sigma(x) = \tanh(x)$.

The bifurcation property is visible in the solution when we consider the properties of $K(k)$, for the minimum value of $K(k)$ is $\pi/2$ at $k = 0$, when $\sigma_R = 0$. Hence, for $n = 1$ in (2.7) the minimum value R_1 of R is given by $R_1 = \pi/2\sqrt{2}$ and for smaller values of R the soliton does not exist except as the constant solution $\sigma = 0$. At the values $R = R_n = nR_1$, $n = 1, 2, \ldots$, there are further bifurcations from $\sigma = 0$ which represent multi-solitons and have n times the energy of a single soliton.

Although a complete description is possible in terms of elliptic functions, including the calculation of the energy, we can detect the presence of the bifurcation in a more general way by linear analysis. To do this we must investigate perturbations about the constant solution $\sigma = 0$ and therefore solve the linearized equation $\sigma'' = -2\sigma$ with $\sigma(0) = 0$. The solution is

$$\sigma(x) = \sin(\sqrt{2}x) \tag{2.8}$$

and $\sigma'(R) = 0$ implies

$$\sqrt{2}R = (2n-1)\frac{\pi}{2} \qquad (n \text{ integer}). \tag{2.9}$$

This shows that a non-trivial solution can bifurcate from $\sigma = 0$ only for the values of R given in (2.9) and accords with R_1 as above. The linearized solution (2.8) also appears correctly as the limit of the general solution (2.6).

This outline indicates how to proceed in the general case when an exact solution is not available, and provides a simple but useful example of how bifurcation occurs in soliton models.

3. Friedberg–Lee model

The Friedberg–Lee model (in three space dimensions) is given by the Lagrangian

$$\mathscr{L} = \bar{\psi}(\mathrm{i}\gamma \cdot \partial - g\sigma)\psi + \tfrac{1}{2}\partial_\mu \sigma \partial^\mu \sigma - U(\sigma) \tag{3.1}$$

where $U(\sigma)$ is the self-energy density of the σ field and g is a coupling constant. We can choose

$$U(\sigma) = B + \frac{a}{2}\sigma^2 + \frac{b}{6}\sigma^3 + \frac{c}{24}\sigma^4 \tag{3.2}$$

where a, b, c and B are constants and $B = U(0)$ is the bag constant. The absolute minimum of $U(\sigma)$ occurs at $\sigma = \sigma_v$ where

$$\sigma_v = \frac{3|b|}{2c}\left[1 + \sqrt{1 - \frac{8ac}{3b^2}}\right]. \tag{3.3}$$

Following Birse *et al* [9] we adopt the Wigner–Seitz approximation, in which the soliton is spherically symmetric and is defined in a sphere of radius R. The field equations reduce to

$$\begin{aligned}
&\frac{\mathrm{d}u}{\mathrm{d}r} = -(\varepsilon + g\sigma)v \\
&\frac{\mathrm{d}v}{\mathrm{d}r} + \frac{2v}{r} = (\varepsilon - g\sigma)u \\
&\frac{\mathrm{d}^2\sigma}{\mathrm{d}r^2} + \frac{2}{r}\frac{\mathrm{d}\sigma}{\mathrm{d}r} = gN(u^2 - v^2) + U'(\sigma)
\end{aligned} \tag{3.4}$$

where N is the number of valence quarks, which we set to three, and the fermion fields are normalized according to

$$4\pi \int_0^R (u^2 + v^2) r^2 \, \mathrm{d}r = 1. \tag{3.5}$$

As in [4] and [10], it is convenient to rescale these equations by putting

$$\begin{aligned}
&r \to rg\sigma_v \qquad \sigma \to \frac{\sigma}{\sigma_v} \qquad \varepsilon \to \frac{\varepsilon}{g\sigma_v} \\
&(u, v) \to \left(\frac{g\sigma_v^3}{N}\right)^{-1/2}(u, v)
\end{aligned} \tag{3.6}$$

and we also put

$$s = \frac{c}{24g^2} \qquad t = -\frac{b}{24g^2\sigma_v} - \frac{a}{4g^2\sigma_v^2}. \tag{3.7}$$

The (rescaled) potential is now

$$U(\sigma) = (\sigma - 1)^2(s\sigma^2 + 2t\sigma + t). \tag{3.8}$$

The equations we wish to solve take the form

$$\begin{aligned}
&\frac{\mathrm{d}u}{\mathrm{d}r} = -(\varepsilon + \sigma)v \\
&\frac{\mathrm{d}v}{\mathrm{d}r} + \frac{2v}{r} = (\varepsilon - \sigma)u \\
&\frac{\mathrm{d}^2\sigma}{\mathrm{d}r^2} + \frac{2}{r}\frac{\mathrm{d}\sigma}{\mathrm{d}r} = u^2 - v^2 + \frac{\mathrm{d}U(\sigma)}{\mathrm{d}\sigma}
\end{aligned} \tag{3.9}$$

with the normalization

$$\int_0^R (u^2 + v^2) r^2 \, \mathrm{d}r = \frac{Ng^2}{4\pi}. \tag{3.10}$$

The boundary conditions are

$$\begin{aligned} &\sigma'(0)=0=\sigma'(R) \\ &v(0)=0=v(R) \end{aligned} \tag{3.11}$$

where we could also have $u(R)=0$ instead of $v(R)=0$ in order to describe quarks at the top of the band.

In order to investigate bifurcation behaviour we must first classify all constant solutions of (3.9), of which there are essentially two possibilities:

$$\sigma=\varepsilon \qquad v=0 \qquad u^2=-U'(\varepsilon) \tag{3.12a}$$

or

$$u=0=v \qquad U'(\sigma)=0. \tag{3.12b}$$

We consider the soliton bag solution, which bifurcates from (3.12a) first. As before, it is convenient to define $s=x/R$ and solve the following equations on $[0, 1]$:

$$\begin{aligned} &\dot{u}=-R(\varepsilon+\sigma)v \\ &\dot{v}+\frac{2v}{s}=R(\varepsilon-\sigma)u \\ &\dot{\sigma}=\tau \\ &\dot{\tau}+\frac{2\tau}{s}=R^2(u^2-v^2)+R^2U'(\sigma) \end{aligned} \tag{3.13}$$

where we have written the equations in first-order form by defining the unknown $\tau=\dot{\sigma}$. Let us denote by z the vector

$$z=\begin{pmatrix} u \\ v \\ \sigma \\ \tau \end{pmatrix}. \tag{3.14}$$

The constant solution is

$$z_0=\begin{pmatrix} \sqrt{-U'(\varepsilon)} \\ 0 \\ \varepsilon \\ 0 \end{pmatrix}. \tag{3.15}$$

The boundary conditions (3.11) may be written

$$\mathbf{P}z(0)=0=\mathbf{P}z(1) \tag{3.16}$$

where the projection matrix $\mathbf{P}$ is given by

$$\mathbf{P}=\begin{pmatrix} 0 & 0 & 0 & 0 \\ 0 & 1 & 0 & 0 \\ 0 & 0 & 0 & 0 \\ 0 & 0 & 0 & 1 \end{pmatrix}. \tag{3.17}$$

We wish to perturb about z_0, and so we substitute $z(s)=z_0+y(s)$, and write (3.13) in the form

$$\dot{y}+\frac{2\mathbf{P}}{s}y=\mathbf{A}y+O(|y|^2). \tag{3.18}$$

The matrix $\mathbf{A}$ is given by $A_{ij}=\partial_j f_i(z_0)$, where f is the vector function on the right-hand side of (3.13), and we find

$$\mathbf{A}=\begin{pmatrix} 0 & -2\varepsilon R & 0 & 0 \\ 0 & 0 & -R\sqrt{-U'(\varepsilon)} & 0 \\ 0 & 0 & 0 & 1 \\ 2R^2\sqrt{-U'(\varepsilon)} & 0 & R^2U''(\varepsilon) & 0 \end{pmatrix}. \tag{3.19}$$

The solution of the equations $\dot{y}+2\mathbf{P}y/s=\mathbf{A}y$ is

$$y(s)=[(\mathbf{A}s)^{-1}-\mathbf{P}(\mathbf{A}s)^{-2}]\,e^{\mathbf{A}s}y(0) \tag{3.20}$$

which can be verified by use of the property

$$\mathbf{AP}+\mathbf{PA}=\mathbf{A}. \tag{3.21}$$

A consequence of this equation is

$$\mathbf{P}f(\mathbf{A})=f(-\mathbf{A})\mathbf{P}+\tfrac{1}{2}[f(\mathbf{A})-f(-\mathbf{A})] \tag{3.22}$$

for any suitable function f.

In order to evaluate the exponential in (3.20) we need to calculate the eigenvalues and eigenvectors of $\mathbf{A}$. The eigenvalues λ are determined by the quartic equation

$$\lambda^4-\lambda^2R^2U''(\varepsilon)+4\varepsilon R^4U'(\varepsilon)=0 \tag{3.23}$$

and hence the eigenvalues come in pairs, $\lambda=\pm\alpha$, $\pm i\beta$, $(\alpha,\beta>0)$, where

$$\alpha^2=\frac{R^2}{2}\left(U''(\varepsilon)+\sqrt{U''(\varepsilon)^2-16\varepsilon U'(\varepsilon)}\right) \tag{3.24a}$$

$$\beta^2=\frac{R^2}{2}\left(-U''(\varepsilon)+\sqrt{U''(\varepsilon)^2-16\varepsilon U'(\varepsilon)}\right). \tag{3.24b}$$

α and β are positive and real provided $\varepsilon>0$ and $U'(\varepsilon)<0$. For each eigenvalue λ there is a corresponding eigenvector ξ_λ given by

$$\xi_\lambda=\begin{pmatrix} 2\varepsilon R^2\sqrt{-U'(\varepsilon)} \\ -\lambda R\sqrt{-U'(\varepsilon)} \\ \lambda^2 \\ \lambda^3 \end{pmatrix}. \tag{3.25}$$

Of interest is the combination $\xi_\lambda+\xi_{-\lambda}$ since it satisfies $\mathbf{P}(\xi_\lambda+\xi_{-\lambda})=0$:

$$\xi_\lambda+\xi_{-\lambda}=\begin{pmatrix} 4\varepsilon R^2\sqrt{-U'(\varepsilon)} \\ 0 \\ 2\lambda^2 \\ 0 \end{pmatrix}. \tag{3.26}$$

The initial and final values $y(0)$ and $y(1)$ are therefore each a linear combination of $\boldsymbol{\xi}_\alpha+\boldsymbol{\xi}_{-\alpha}$ and $\boldsymbol{\xi}_{i\beta}+\boldsymbol{\xi}_{-i\beta}$, in particular

$$y(0)=c_1(\boldsymbol{\xi}_\alpha+\boldsymbol{\xi}_{-\alpha})+c_2(\boldsymbol{\xi}_{i\beta}+\boldsymbol{\xi}_{-i\beta}). \tag{3.27}$$

We must also impose $\mathbf{P}y(1)=0$ and since (from (3.20))

$$y(1)=(\mathbf{A}^{-1}-\mathbf{A}^{-2}\sinh\mathbf{A})y(0) \tag{3.28}$$

we find

$$0=\mathbf{P}y(1)=(\mathbf{A}^{-1}\cosh\mathbf{A}-\mathbf{A}^{-2}\sinh\mathbf{A})y(0) \tag{3.29}$$

or

$$(\mathbf{A}-\tanh\mathbf{A})y(0)=0. \tag{3.30}$$

On substituting for $y(0)$ from (3.27) we find that $c_1=0$, since we cannot satisfy $\alpha=\tanh\alpha$ non-trivially, and β must satisfy $\tan\beta=\beta$. This equation has an infinite number of solutions, $\beta_1=4.4934,\ldots,\beta_2=7.725,\ldots$, and an approximate solution, valid for large integers n, is

$$\beta_n=(n+\tfrac{1}{2})\pi-\frac{1}{(n+\frac{1}{2})\pi}. \tag{3.31}$$

For each such β_n there is a corresponding radius R_n determined from (3.24*b*).

We have obtained, therefore, a necessary condition for the existence of solutions bifurcating from the constant solution (3.12*b*), i.e. the bifurcation takes place only when the radius R attains one of the values R_n and in this case the linearized solution is given by (3.20), with $y(0)=\boldsymbol{\xi}_{i\beta_n}+\boldsymbol{\xi}_{-i\beta_n}$. For other values of R, away from the bifurcation radius, the solution must be calculated numerically from the nonlinear equations (3.13). The existence of multiple bifurcation points reflects the existence of multi-soliton solutions, as in one dimension, except that here these solutions cannot be obtained by simply joining together single soliton solutions.

In order to obtain R_n in terms of the physical parameters we must eliminate the eigenvalue ε by using the normalization (3.10). At $R=R_n$ we have (since $v=0$ and $u^2=-U'(\varepsilon)$)

$$\frac{3Ng^2}{4\pi}=-U'(\varepsilon)R^3. \tag{3.32}$$

This equation, together with (3.24*b*), enables us to express ε in terms of Ng^2 and the parameters of U. By eliminating square roots we find

$$\beta^6(U')^2-G(12\varepsilon U'U''-(U'')^3)+64\varepsilon^3\beta^{-6}G^2U'=0 \tag{3.33}$$

where $G=(3Ng^2/4\pi)^2$. If U is a fourth-order polynomial in ε then (3.33) is a sixth-order polynomial equation in ε, which is easily solved numerically, given G and U, for one of the possible values of β. In general there can be spurious solutions to (3.33); however, we have found that there appears to be always only one genuine solution. This contrasts with the one-dimensional case for which two solutions exist, leading to the shallow and deep bags [11].

For the choice (3.7) of U we can always find a solution for large Ng^2, corresponding to a value of ε near 1. To leading order in Ng^2 we find:

$$1-\varepsilon=\left(\frac{\beta^2}{4}\right)^3\left(\frac{4\pi(6t+2s)}{3Ng^2}\right)^2+\ldots \tag{3.34}$$

and the corresponding radius is

$$R = \frac{3Ng^2}{\beta^2\pi(6t+2s)} + \ldots \tag{3.35}$$

There are two cases for which explicit solutions are possible, these occurring when $(U'')^2 - 16\varepsilon U'$ is a perfect square. The two cases are

(a) $s = \frac{1}{2} = t$, for which

$$\varepsilon = \sqrt{\frac{2G}{2G+\beta^6}} \qquad R = \sqrt{\frac{\beta^2}{2} + \frac{G}{\beta^4}} \tag{3.36}$$

(b) $s = \frac{1}{2}$, $t = \frac{1}{6}$, for which

$$\varepsilon = \frac{16G}{16G+\beta^3} \qquad R = \frac{3Ng^2}{2\pi\beta^2} + \frac{\pi\beta^4}{6Ng^2}. \tag{3.37}$$

This latter case is perhaps of some physical interest, since the parameters are close to those previously used to model the nucleon (see parameter set (i) below). It should be noted that, unlike the case of one dimension, it is not necessarily true that the bifurcation radii $R_1, R_2 \ldots$ are ordered, $R_1 < R_2 < R_3 \ldots$. That this is possible is clear from both (3.36) and (3.37), since for small β, R decreases as β increases.

We give three examples for which we have calculated the values of the bifurcation radius; the first two parameter sets have been used by Achtzehnter *et al* [12] and satisfy $a = 0$, implying that $s = 3t$ and $\sigma_v = -3b/c$, while the third set is used in [13]. The parameter sets and results are:

(i) $g = 9.037$, $a = 0$, $b = -105.14\ \mathrm{fm}^{-1}$ and $c = 1000$ for which $s = 0.5102$ and $t = 0.170\,07$. We find that $R_1 = 2.31$ fm ($\varepsilon = 0.866$), $R_2 = 3.32$ fm ($\varepsilon = 0.207$) and $R_3 = 10.74$ fm ($\varepsilon = 0.032$), where ε is the dimensionless eigenvalue rescaled as in (3.6).

(ii) $g = 19.357$, $a = 0$, $b = -7482.4\ \mathrm{fm}^{-1}$ and $c = 200\,000$ for which $s = 22.24$ and $t = 7.413$. We find that $R_1 = 1.267$ fm ($\varepsilon = 0.725$), $R_2 = 1.258$ fm ($\varepsilon = 0.645$) and $R_3 = 1.277$ fm ($\varepsilon = 0.579$).

(iii) $g = 25$, $a = 236.13$, $b = -11\,614\ \mathrm{fm}^{-1}$ and $c = 180\,000$ for which $s = 12$ and $t = 0.568\,47$. We find that $R_1 = 1.75$ fm ($\varepsilon = 0.89$), $R_2 = 1.5897$ fm ($\varepsilon = 0.79$) and $R_3 = 1.5898$ fm ($\varepsilon = 0.74$).

These values of R_1 give approximately the radius at which the overlapping solitons cease to exist as distinct entities although this is determined accurately only from precise numerical solutions as found in section 5. By comparison it was found in [12], where the equations of the model were solved on a crystal lattice, that the corresponding values of R were 3 and 2.1 fm for the first two parameter sets above, whereas we obtained 2.3 and 1.3 fm respectively.

It is also possible to have soliton bag solutions satisfying $u(R) = 0$ instead of $v(R) = 0$. For this case β is no longer determined by the simple equation $\tan\beta = \beta$; instead there is a transcendental equation involving both α and β which implicitly determines R. The linearized solution is found as previously, and bifurcation occurs in the same way.

4. Kink solitons

Apart from the soliton bag there is another type of solution, which we refer to as the kink soliton, which bifurcates from a constant solution different to that for the soliton bag. Such solutions with similar bifurcation behaviour also occur in one-dimensional models [14] where they are the familiar kink solutions. The constant solutions are given in (3.12) and for the second possibility we have $U'(\sigma)=0$, implying $\sigma=1$, $\sigma=0$ or $\sigma=(s-3t)/2s$. The first solution corresponds to the vacuum and can be ignored since it does not give rise to solitons. It will be seen that a non-trivial solution bifurcates from one of the other solutions, specifically from the larger of 0 and $(s-3t)/2s$, corresponding to the central hump in the potential $U(\sigma)$. We find it convenient to solve the nonlinear equations keeping ε fixed, which means that along a solution branch with ε held constant the parameter Ng^2 will vary. In particular at the bifurcation point where $u=0=v$ we must have $Ng^2=0$ (from (3.10)). Conversely, if we follow a solution branch keeping Ng^2 fixed (and non-zero) we cannot reach the bifurcation point which is therefore unphysical. Numerically, by keeping ε fixed we can follow the non-trivial bifurcation branch and when Ng^2 is non-zero follow the branch for varying ε and fixed Ng^2.

Suppose that $s-3t<0$ and let us investigate the bifurcation about $\sigma=0=u=v$. We may assume $0\leqslant t\leqslant s$ and so $\sigma=0$ corresponds to the central (local) maximum of $U(\sigma)$. We first determine values of R for which the linearized equations possess solutions. The linearized equations for u and v are

$$\frac{\mathrm{d}u}{\mathrm{d}r}+\varepsilon v=0=\frac{\mathrm{d}v}{\mathrm{d}r}+\frac{2v}{r}-\varepsilon u \tag{4.1}$$

for which the solutions are

$$\begin{aligned} u&=\mu\frac{\sin\varepsilon r}{r}\\ v&=\mu\left(\frac{\sin\varepsilon r}{\varepsilon r^2}-\frac{\cos\varepsilon r}{r}\right)\end{aligned} \tag{4.2}$$

where μ is arbitrary. (Here we have chosen the solution for u which is regular at the origin, and then the condition $v(0)=0$ is satisfied.) If we apply the boundary conditions $v(R)=0$ we find $\tan\varepsilon R=\varepsilon R$ so that solutions exist only for $\varepsilon R_n=\beta_n$ where $\tan\beta_n=\beta_n$. In this way we have expressed the bifurcation radius, for kink solitons, in terms of the given eigenvalue ε.

We still need to solve the linearized σ equation. Since u and v have been determined, u^2-v^2 is fixed and we must solve

$$\frac{\mathrm{d}^2\sigma}{\mathrm{d}r^2}+\frac{2}{r}\frac{\mathrm{d}\sigma}{\mathrm{d}r}+2(3t-s)\sigma=u^2-v^2. \tag{4.3}$$

It is convenient to define $w=r\sigma+ru^2/2\varepsilon^2$, then

$$\frac{\mathrm{d}^2w}{\mathrm{d}r^2}+c^2w=\mu^2c^2\frac{\sin^2\varepsilon r}{2\varepsilon^2 r} \tag{4.4}$$

where $c^2=2(3t-s)$. The general solution is the sum of a special solution and the general solution to the homogeneous equation. In order to find a special solution we use Lagrange's method of variation of parameters, outlined for example in Kreyszig [15, p 122]. Define

$$\begin{aligned} f(r)&=\frac{c}{2\varepsilon^2}\int_0^r\frac{\cos cr\sin^2\varepsilon r}{r}\,\mathrm{d}r\\ g(r)&=-\frac{c}{2\varepsilon^2}\int_0^r\frac{\sin cr\sin^2\varepsilon r}{r}\,\mathrm{d}r\end{aligned} \tag{4.5}$$

then f and g satisfy $f' \sin cr + g' \cos cr = 0$. These functions are related to the sine and cosine integrals defined, for example, in Abramowitz and Stegun [8, ch 5]. Explicitly,

$$
\begin{aligned}
f(r) &= \frac{c}{8\varepsilon^2}(2\,\mathrm{Ci}(cr) - \mathrm{Ci}(|c+2\varepsilon|r) - \mathrm{Ci}(|c-2\varepsilon|r)) \\
g(r) &= -\frac{c}{8\varepsilon^2}(2\,\mathrm{Si}(cr) - \mathrm{Si}((c-2\varepsilon)r) - \mathrm{Si}(c+2\varepsilon)r).
\end{aligned}
\tag{4.6}
$$

A special solution to (4.4) is

$$w = \mu f(r) \sin cr + \mu g(r) \cos cr. \tag{4.7}$$

From this we construct a general solution of (4.3):

$$\sigma = -\frac{u^2}{2\varepsilon^2} + \mu^2 A \frac{\sin cr}{r} + \mu^2 f(r) \frac{\sin cr}{r} + \mu^2 g(r) \frac{\cos cr}{r} \tag{4.8}$$

where u is given in (4.2), and A is a constant. This solution satisfies $\sigma'(0) = 0$ and we must also impose $\sigma'(R) = 0$, which determines A:

$$A = -f(R) + g(R) \frac{cR \sin cR + \cos cR}{cR \cos cR - \sin cR} \tag{4.9}$$

where R takes one of the values $R_n = \beta_n/\varepsilon$. This completes the evaluation of the linearized solution bifurcating from $\sigma = 0 = u = v$.

We have considered only the case $s - 3t < 0$, but expect that for $s - 3t > 0$ the bifurcation will take place from $u = v = 0$, $\sigma = (s-3t)/2s$. In the limit $R \to \infty$ we would not expect the kink soliton to survive since in three dimensions it cannot retain its finite energy. Further study of these solutions is required, in particular it remains to calculate the energies of both bag and kink solitons for a given R to determine which has the lower energy.

5. Numerical method and results

Given the necessary conditions for the existence of a bifurcation and the linearized solution at $R = R_n$ we can numerically calculate the solution of the full nonlinear equations for values of R near R_n. By continuation this solution can be found for arbitrary values of R and also for other values of the parameters in the equations. A method was described in [4] for obtaining accurate numerical solutions to soliton bag models. The system of coupled equations is treated as a two-point boundary value system, with the normalization condition converted to a differential equation with associated boundary conditions. Standard library routines can solve the system to high accuracy provided a reasonable initial guess is known. We will solve the system for a fixed eigenvalue ε, following Köppel and Harvey [10]. This permits greater simplicity since there are fewer equations because the normalization is ignored, and the parameter Ng^2 is then calculated after the solution is found. Furthermore, it is essential to allow Ng^2 to vary in order to numerically find the kink soliton bifurcating from $u = 0 = v$, as explained in section 4. Once a solution is obtained away from the bifurcation point, sufficiently far so that convergence is not affected by the presence of a nearby solution, we can revert to the method of [4] and follow the solution branch for constant Ng^2, while varying R and consequently ε. The numerical method we describe does not require an accurate initial guess, unlike that in [4] and [10], and can therefore be used to generate solutions for arbitrary values of R without prior knowledge of the solution.

The method is similar to that used to compute periodic solutions arising from a Hopf bifurcation, and has been described by Weber [16]. The difficulty to be overcome is to ensure that the method follows the non-trivial branch from the bifurcation point, avoiding the constant solution, and this is achieved by imposing an orthogonality condition. In general, we are given a constant solution z_0 and the linearized solution $y(s)$, $0 \leqslant s \leqslant 1$, valid for some radius R. We seek solutions to (3.13) in the form

$$z(s) = z_0 + \mu y(s) + \mu^2 \boldsymbol{\phi}(\mu, s) \tag{5.1}$$

where μ is a perturbation parameter to be determined and $\boldsymbol{\phi}$, which depends on μ as well as s, is the new unknown. By varying μ we follow the solution branch away from the bifurcation point $\mu = 0$. The radius is therefore also given in terms of μ:

$$R(\mu) = R + \mu\rho(\mu) \tag{5.2}$$

where ρ, which depends on μ, is the unknown. To ensure that we avoid the constant solution we impose

$$\int_0^1 y(s) \cdot \boldsymbol{\phi}(s)\, \mathrm{d}s = 0. \tag{5.3}$$

It is convenient to convert the integral condition to a differential equation with endpoint conditions, thereby writing the equations as a two-point boundary value system. Define therefore

$$\zeta(s) = \int_0^s y(s) \cdot \boldsymbol{\phi}(s)\, \mathrm{d}s \tag{5.4}$$

which satisfies

$$\dot{\zeta} = y \cdot \boldsymbol{\phi} \tag{5.5}$$

with the boundary conditions

$$\zeta(0) = \zeta(1) = 0. \tag{5.6}$$

From (5.2) we also have

$$\dot{\rho} = 0. \tag{5.7}$$

The boundary conditions for $\boldsymbol{\phi}$ follow from (3.1) and the properties of the linearized solution y and so we must have

$$\bar{\mathbf{P}}\boldsymbol{\phi}(0) = 0 = \bar{\mathbf{P}}\boldsymbol{\phi}(1). \tag{5.8}$$

We therefore have six unknowns, $\boldsymbol{\phi}$, ρ, ζ, and six equations to solve, these being (3.13), (5.5) and (5.7) together with six boundary conditions, namely two in (5.6) and four in (5.8). The equations for $\boldsymbol{\phi}$ are found from (3.13) upon substituting for $z(s)$ as shown in (5.1). The equations are expressed as a two-point boundary value system of order 6 which we solve by standard numerical routines, for some small value of μ. We found that the initial guess $\boldsymbol{\phi} = 0 = \zeta = \rho$ was satisfactory in all cases, leading to rapid convergence. The algorithm will converge provided that μ is sufficiently small [16] and, because of the orthogonality condition, (5.4) will provide a non-trivial solution branch. From a solution $\boldsymbol{\phi}$, ρ we obtain u, v, σ and R from (5.1) and (5.2) and the parameter Ng^2 is calculated from (3.10). We generate the complete solution branch by continuation in μ, i.e. we choose successively larger values of μ and solve using the previous solution as an initial guess. When R has increased sufficiently we can revert to the previous method [4, 10].

For the soliton bag $y(s)$ is obtained from (3.20) and is given by

$$y(s)=\begin{pmatrix} 2\varepsilon R^2\dfrac{\sin\beta s}{\beta s}\sqrt{-U'(\varepsilon)} \\ R\sqrt{-U'(\varepsilon)}\left(\dfrac{\sin\beta s}{\beta s^2}-\dfrac{\cos\beta s}{s}\right) \\ -\dfrac{\beta\sin\beta s}{s} \\ \dfrac{\beta\sin\beta s}{s^2}-\dfrac{\beta^2\cos\beta s}{s} \end{pmatrix}. \tag{5.9}$$

In this expression ε is fixed, β is a solution of $\tan\beta=\beta$, and R is obtained from (3.24*b*).

For the kink solitons of section 4 the method must be modified slightly to take account of the different form of the linearized solution. The constant solution is $z_0=0$ and u and v are written in the form (5.1):

$$\begin{aligned} u&=\mu y_1+\mu^2\phi_1 \\ v&=\mu y_2+\mu^2\phi_2 \end{aligned} \tag{5.10}$$

where y_1 and y_2 can be identified from (4.2). However the linearized solution for σ (4.8) shows that σ must be written

$$\sigma=\mu^2 y_3+\mu^3\phi_3 \tag{5.11}$$

where y_3 can be identified from (4.8). ρ and ζ are defined as before in (5.2) and (5.4). Again, we choose some small μ, having fixed ε, and solve the two-point boundary value system with the initial guess $\boldsymbol{\phi}=0=\rho=\zeta$.

In practice, the numerical scheme worked efficiently and we were able to obtain accurate solutions for both the soliton bag and kink solitons near the relevant bifurcation point. We chose values for s, t and ε and calculated solutions bifurcating from each of $R=R_1$, R_2. Figure 1 shows a plot of the field energy E against R for the two choices $s=8$, $t=0.5$, $\varepsilon=0.8$ and $s=10$, $t=1$, $\varepsilon=0.77$ with the bifurcation points labelled R_1 and R_1' respectively. E and R are dimensionless, scaled as indicated in (3.6), and the bifurcation radii are $R_1=3.55$ and $R_1'=3.035$. The constant solution, for each set of parameters, has an energy proportional to R^3 and is shown by a dotted curve (when visible) for each case. As μ is increased from zero, R at first decreases with the bag having a higher energy than that of the constant solution. At a minimum value $R=2.37$ (respectively 2.037) the curve has a cusp, following which both R and E increase with μ. At $R=2.48$ (respectively 2.14) the curve crosses that for the constant solution and consequently for larger R the soliton bag has lower energy than that of the constant solution. In other words, if we begin with a soliton bag solution for large R and then decrease R the field configuration of lowest energy changes discontinuously from the soliton bag (the nucleon) to a constant (the uniform plasma) at the point where the solution branches cross. Figure 2 shows a plot of the solution at $R=4.14$, well away from the bifurcation point, for $s=8$, $t=0.5$ and $\varepsilon=0.8$, and shows u, v and σ as functions of r (dimensionless, scaled as in (3.6)). The fact that $u(R)$ is not small indicates that for the fermion fields there is some overlap with adjoining soliton bags; however, the σ field almost reaches its vacuum value at $r=R$.

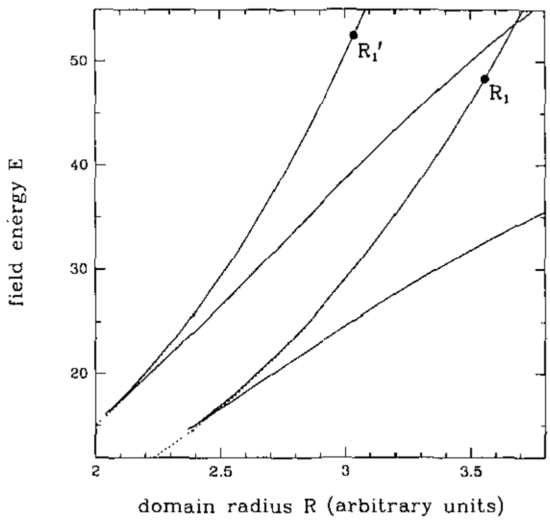

Figure 1. Energy against R curves for the two parameter sets $s = 8$, $t = 0.5$, $\varepsilon = 0.8$ (passing through the bifurcation point R_1) and $s = 10$, $t = 1$, $\varepsilon = 0.77$ (passing through R_1'). The constant solutions are shown by dotted lines and two bifurcating branches are shown at each of R_1 and R_1'.

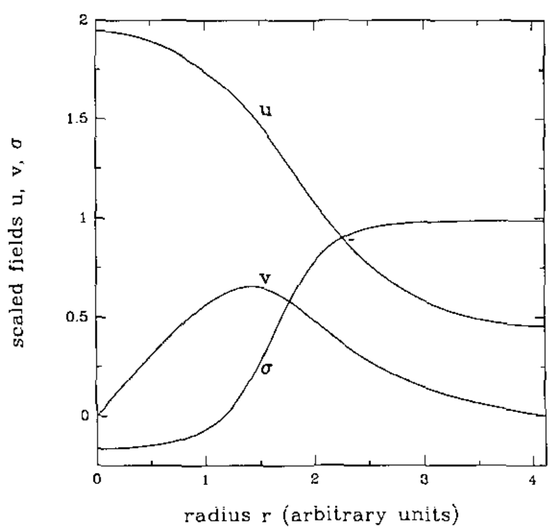

Figure 2. The fields u, v and σ as functions of r for the soliton bag with $s = 5$, $t = 0.2$, $\varepsilon = 0.8$, $R = 4.14$ and $g = 7.77$.

Figure 1 shows that there is another solution branch bifurcating from R_1 (and R_1'), obtained by choosing negative values for μ. As μ is decreased from zero, R increases as shown in figure 1 by the curves which bifurcate from R_1 and R_1' to the right. These solutions have energy slightly less than those of the constant solutions, although this is not visible in figure 1. These curves also describe soliton bags, but ones which are 'inverted'. The solution for $R = 6$, $s = 8$ and $t = 0.5$, with $\varepsilon = 0.74$ and $g = 30$ is shown in figure 3 and we describe it as inverted because σ is close to its vacuum value **1** in the interior of the bag, so that its energy resides mainly in a shell on the surface at

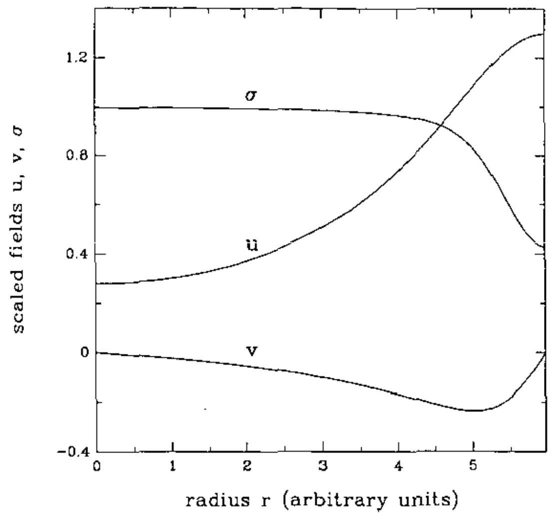

Figure 3. An 'inverted' soliton showing the fields u, v and σ as functions of r for $s=8$, $t=0.5$, $\varepsilon=0.74$, $R=6$ and $g=30$.

$r=R$. This solution has a one-dimensional analogue. We found that as R was increased the numerical algorithm failed to converge at approximately $R=8.8$ (for $g=30$, $s=8$, $t=0.5$).

The bifurcations shown in figure 1 are repeated at a second value $R=R_2$ with two branches extending either side of the bifurcation point. These branches also have one-dimensional analogues and describe in this case a two-soliton solution. In one dimension we can construct such solutions simply by joining together two single solitons, reflecting the translational invariance of the one-dimensional model. Here, the equations are not invariant under translations in r; however, the 'translated' solutions still exist, at least for small R. Figure 4 shows the two-soliton solution at

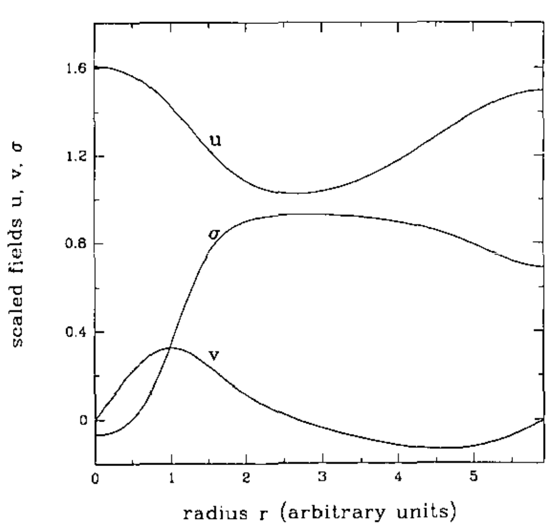

Figure 4. A double-soliton bifurcating from $R_2=6.11$ showing the fields u, v and σ as functions of r for $s=8$, $t=0.5$, $\varepsilon=0.8$, $R=5.96$ and $g=22.66$.

$R=5.96$ on the branch bifurcating to the left, for the parameters $s=8$, $t=0.5$ and $\varepsilon=0.8$. The solution evidently is composed of a single soliton bag for $r\leqslant 2.66$, surrounded by an inverted soliton for $2.66\leqslant r\leqslant 5.96$ which resembles a translated inverted soliton as in figure 3. The solution describes two superimposed solitons located at the same point, one inside the other. We found numerically that this solution appears not to exist for R larger than about 8.5. There is also a branch bifurcating from $R=R_2$ to the right which is obtained by allowing μ to take negative values. Figure 5 provides an example of such a solution, for $s=8$, $t=0.5$ and $\varepsilon=0.75$ (giving $g=31.8$) with $R=8$. Here, the inverted soliton is enclosed by a soliton bag with the transition between the two occurring at $r=6.25$.

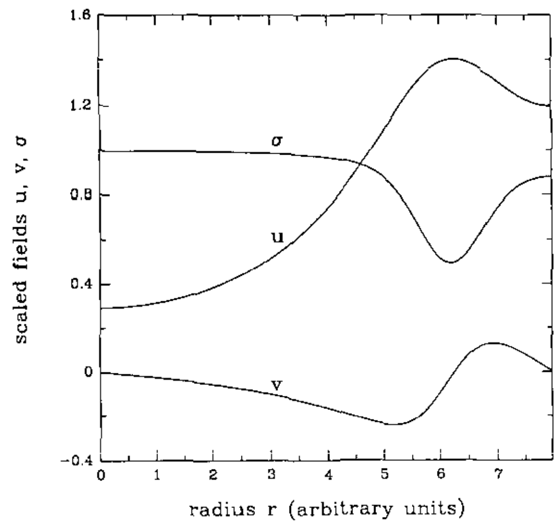

Figure 5. A double-soliton (second branch) bifurcating from $R_2=6.11$ showing the fields u, v and σ as functions of r for $s=8$, $t=0.5$, $\varepsilon=0.75$, $R=8$ and $g=31.8$.

Apart from the soliton bags there are the kink solutions described in section 4. We have not systematically determined the energies of these solutions relative to the soliton bag, to find which has the lower energy; however, some examples indicate their energy is higher. Solutions were calculated in the way described earlier, and an example is shown in figure 6 with $s=2$, $t=1$, $\varepsilon=0.8$, $R=5.64$. The bifurcation radius R_1 for these parameters is 5.617, close to $R=5.64$, and so there is only a small variation in the range of u, v, σ and g is small. Further numerical investigation is required in order to determine other properties of these three-dimensional kink solitons, including the range of values of R for which they exist.

In conclusion, we have demonstrated that the Friedberg–Lee model has a rich set of soliton solutions for small R, when the solutions are confined to a sphere of radius R. We have obtained these solutions not by continuation from those at $R=\infty$, but as branches bifurcating from the constant solutions with R being the bifurcation parameter. By numerical calculation we have determined the branches of lowest energy and found that at a certain value of R the lowest energy solution changes discontinuously from a soliton bag to a constant solution. In the mean field approximation these solutions are relevant to the quantum theory, and indeed it has been argued by Cohen [17] that the accuracy of this approximation is greater at high nucleon densities.

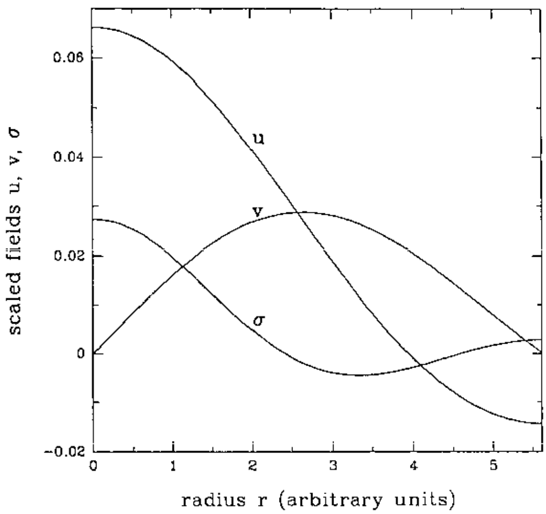

Figure 6. A kink-soliton bifurcating from $R_1 = 5.617$ showing the fields u, v and σ as functions of r for $s = 2$, $t = 1$, $\varepsilon = 0.8$, $R = 5.64$ and $g = 0.39$.

We interpret therefore the discontinuity when solution branches cross as describing a transition from the nucleon state to a uniform fermion-scalar field plasma. The methods we have used are general and will apply to generalizations of the Friedberg–Lee model such as the chromo-dielectric model [1], and can also be used to investigate the case when fermions occupy excited levels, corresponding to nucleons at non-zero temperature.

Acknowledgment

This work has been partially supported by the Australian Research Council.

References

[1] Wilets L 1989 *Nontopological Solitons* (Singapore: World Scientific)
[2] Friedberg R and Lee T D 1977 *Phys. Rev.* D **15** 1694; 1977 *Phys. Rev.* D **16** 1096; 1978 *Phys. Rev.* D **18** 2623
[3] Lee T D 1981 *Particle Physics and Introduction to Field Theory* (Chur, Switzerland: Harwood Academic)
[4] Dodd L R and Lohe M A 1986 *Phys. Rev.* D **32** 1816
[5] Dodd L R and Lohe M A Exact solutions for a soliton crystal *Preprint* University of Adelaide
[6] Reiss E L 1969 *Bifurcation Theory and Nonlinear Eigenvalue Problems* ed J B Keller and S Antman (Amsterdam: Benjamin)
[7] Chow S-N and Hale J K 1982 *Methods of Bifurcation Theory* (New York: Springer)
[8] Abramowitz M and Stegun I A 1965 *Handbook of Mathematical Functions* (New York: Dover)
[9] Birse M C, Rehr J J and Wilets L 1988 *Phys. Rev.* C **38** 359
[10] Köppel Th and Harvey M 1985 *Phys. Rev.* D **31** 171
[11] Dodd L R, Lohe M A and Rossi M 1987 *Phys. Rev.* C **36** 1573
[12] Achtzehnter J, Scheid W and Wilets L 1985 *Phys. Rev.* D **32** 2414
[13] Goldflam R and Wilets L 1984 *Comm. Nucl. Phys.* **12** 191
[14] Lohe M A Bifurcation of soliton bags: two-dimensional linear σ model *Preprint*
[15] Kreyszig E 1983 *Advanced Engineering Mathematics* 5th edn (New York: Wiley)
[16] Weber H 1980 *Math. Meth. Appl. Sci.* **2** 178
[17] Cohen T D 1989 *Nucl. Phys.* A **495** 545